Journal of Quantitative Spectroscopy & Radiative Transfer 175 (2016) 1–7

Contents lists available at ScienceDirect

Journal of Quantitative Spectroscopy & Radiative Transfer

journal homepage: www.elsevier.com/locate/jqsrt

Global modeling of the $^{15}N_2{}^{16}O$ line positions within the framework of the polyad model of effective Hamiltonian and a room temperature $^{15}N_2{}^{16}O$ line list

S.A. Tashkun [a,b,*], V.I. Perevalov [a], A.-W. Liu [c], S.-M. Hu [c]

[a] Laboratory of Theoretical Spectroscopy, V.E. Zuev Institute of Atmospheric Optics, Siberian Branch, Russian Academy of Sciences, Academician Zuev square 1, Tomsk 634055, Russia

[b] Laboratory of Climate and Environmental Physics, Ural Federal University, Mira street, 19, Yekaterinburg 620002, Russia

[c] Hefei National Laboratory for Physical Sciences at Microscale, Department of Chemical Physics, University of Science and Technology of China, Hefei 230026, China

ARTICLE INFO

Article history:
Received 21 December 2015
Received in revised form
28 January 2016
Accepted 28 January 2016
Available online 3 February 2016

Keywords:
Nitrous oxide
$^{15}N_2{}^{16}O$
Global modeling
GEISA
Line list

ABSTRACT

The global modeling of $^{15}N_2{}^{16}O$ line positions in the 4–12,516 cm^{-1} region has been performed using the polyad model of effective Hamiltonian. The effective Hamiltonian parameters were fitted to the line positions collected from an exhaustive review of the literature. The dimensionless weighted standard deviation of the fit is 1.31. The fitted set of 109 parameters allowed reproducing more than 18,000 measured line positions with an RMS value of 0.001 cm^{-1}. A line list was calculated for a reference temperature 296 K, natural abundance (1.32×10^{-5}), and an intensity cutoff 10^{-30} cm/molecule. The line list is based on the fitted set of the effective Hamiltonian parameters for $^{15}N_2{}^{16}O$ obtained in this work and the effective dipole moment parameters of the $^{15}N_2{}^{16}O$ and $^{14}N_2{}^{16}O$ isotopologues. Accurate values of the $^{15}N_2{}^{16}O$ total partition function are also given.

1. Introduction

Nitrous oxide, N_2O, is a minor constituent of the Earth atmosphere but it plays an important role in atmospheric physics and chemistry. Being a green house gas it contributes to the atmospheric radiation balance. Through the atmospheric chemistry processes N_2O participates to the ozone layer depletion. In addition, nitrous oxide is one of the products of the burning of the organic fuels in air.

There are 12 stable isotopic species of N_2O formed by ^{14}N, ^{15}N, ^{16}O, ^{17}O, and ^{18}O atoms. Six of them are isotopomers ($^{14}N^{15}N^{16}O$ and $^{15}N^{14}N^{16}O$, $^{14}N^{15}N^{18}O$ and $^{15}N^{14}N^{18}O$, $^{14}N^{15}N^{17}O$ and $^{15}N^{14}N^{17}O$) and the others are isotopologues ($^{14}N_2{}^{16}O$, $^{15}N_2{}^{16}O$, $^{14}N_2{}^{18}O$, $^{15}N_2{}^{18}O$, $^{14}N_2{}^{17}O$, and $^{15}N_2{}^{17}O$). Terrestrial abundances of all isotopic species can be calculated as products of respective atomic abundances [1]. In Table 1 we list first six most abundant isotopic species along with abundances taken from the HITRAN database [2] and calculated from the atomic abundances.

Isotopic species, which contain ^{15}N are important both for atmospheric and bioorganic applications [3] and geochemistry [4]. Measuring their concentrations in the atmosphere and in minerals it is possible to determine the value of $\delta^{15}N$, which denotes the relative difference in per mil (‰) of the $^{15}N/^{14}N$ ratio of the sample versus the reference material. In particular, $\delta^{15}N$ can provide an important insight into understanding N_2O atmospheric sources and sinks. At present time, the $\delta^{15}N$ values are derived from the detection of $^{14}N^{15}N^{16}O$ and $^{15}N^{14}N^{16}O$ in the atmosphere with quantum cascade laser based

* Corresponding author at: Laboratory of Theoretical Spectroscopy, V.E. Zuev Institute of Atmospheric Optics, Siberian Branch, Russian Academy of Sciences, Academician Zuev square 1, Tomsk 634055, Russia.
E-mail address: tashkun@rambler.ru (S.A. Tashkun).

http://dx.doi.org/10.1016/j.jqsrt.2016.01.038
0022-4073/

Table 1
Abundances of the most abundant isotopic species of N_2O.

Isotope	HITRAN abundance	Product of atomic abundances
$^{14}N_2^{16}O$	0.9903	0.9903
$^{14}N^{15}N^{16}O$, $^{15}N^{14}N^{16}O$	3.641E−3	3.618E−3
$^{14}N_2^{18}O$	1.986E−3	2.035E−3
$^{14}N_2^{17}O$	3.693E−4	3.772E−4
$^{15}N_2^{16}O$		1.321E−5

absorption spectroscopy [5]. From the other side, the $\delta^{15}N$ values and the constants of the isotope exchange reactions involving ^{15}N containing isotopic species [4] could be found from an analysis of the $^{15}N_2^{16}O$ spectra. For this purpose it is necessary to know the line positions and intensities of rovibrational $^{15}N_2^{16}O$ lines in the infrared as well as accurate values of the $^{15}N_2^{16}O$ partition function $Q(T)$ at different temperatures.

Up to now there are only a few studies dealing with measurements of the line positions [6–13] and line intensities [10,12,14]. $^{15}N_2^{16}O$ data are absent in the HITRAN database [2], but present in the GEISA database [15] and in Toth's line list sisam.n2o of N_2O parameters from 500 to 7500 cm^{-1} [14]. The line list contains 424 lines of the 00011-00001, 01111-01101, 01112-01102, 10001-00001, 10011-00001, and 20001-00001 bands in the 1227–3415 cm^{-1} spectral range. GEISA contains 455 lines of the same bands. The line intensities of these bands cover the 10^{-23}–10^{-25} cm/molecule interval. Here we use for an energy level the notation adopted in the HITRAN and GEISA databases $V_1V_2l_2V_3w$, where V_1, V_2, and V_3 denote the normal mode vibrational quantum numbers, l_2 is the vibrational angular momentum quantum number and w is the Wang parity $w=1$ for the e type levels and $w=2$ for the f type levels, respectively. To meet the needs of possible applications the modern spectroscopic databases [2,15] collect parameters of the lines with intensity cutoff 10^{-30} cm/molecule. The positions and intensities of $^{15}N_2^{16}O$ lines with intensities below 10^{-25} cm/molecule could be obtained as a result of the theoretical modeling.

There are two approaches used for theoretical modeling of high resolution spectra. One of them is based on the variational principle and a potential energy surface (PES) to calculate the line positions and on a dipole moment surface (DMS) to calculate the line intensities. PES can be obtained either from pure *ab initio* calculations or from a fit to the experimental energy levels or line positions. Teffo and Chedin [16] constructed a PES expanded with respect to the mass-independent quasi-normal internal coordinates. PES expansion coefficients were fitted to 267 band centers (G_v), 319 rotational constants (B_v), and 333 centrifugal distortion constants (H_v) belonging to the $^{14}N_2^{16}O$, $^{14}N^{15}N^{16}O$, $^{15}N^{14}N^{16}O$, $^{14}N_2^{18}O$, $^{15}N_2^{16}O$, and $^{15}N_2^{18}O$. The vibrational band centers were fitted with RMS= 0.047 cm^{-1}. Based on the fitted PES, molecular and spectroscopic parameters of 12 isotopologues were computed up to 4th order of the perturbation theory. Recently, Schroder et al. [17] published a high-level *ab initio* PES and DMS. Zúñiga et al. [18] presented variational calculations of the spectroscopic constants G_v and B_v of $^{14}N^{15}N^{16}O$, $^{15}N^{14}N^{16}O$ and $^{15}N_2^{16}O$. The constants were calculated using normal hyperspherical coordinates and the Morse-cosine N_2O PES previously determined by the authors. The PES has good isotopic extrapolation properties. All G_v constants of the $^{15}N_2^{16}O$ states with $l_2<5$ having energies up to 13,000 cm^{-1} differ from the experimental values by less than 1 cm^{-1}. However, the absence of the centrifugal distortion constants H_v limits applicability of the calculated line positions to low J values.

Over the years, we use another theoretical approach which enables us to model the line positions of CO_2 and N_2O with a spectroscopic level of accuracy ($\sim$0.001 cm^{-1}). It is based on the effective operators approach and is adopted for the global description of the energy levels and transition probabilities inside a given electronic state. In particular, we have successfully applied this method to the global modeling of the line positions [19] and the line intensities [20–27] of the principal isotopologue, $^{14}N_2^{16}O$, and to the global modeling of the line positions of the rare isotopic species $^{14}N^{15}N^{16}O$ and $^{15}N^{14}N^{16}O$ [28], $^{14}N_2^{18}O$ and $^{14}N_2^{17}O$ [29], $^{15}N_2^{16}O$ [10].

The set of effective Hamiltonian parameters obtained in 2010 for $^{15}N_2^{16}O$ [10] allowed us predicting the line positions in a wide spectral range. These predictions were used for the assignment of the spectra recorded by Fourier transform spectroscopy (FTS) [11,13] and continuous wave cavity ring down spectroscopy (CW-CRDS) [12]. Since 2010, the amount of the observed data has been considerably extended. Details of the observed data are discussed in Section 3.

The purpose of this paper is, (i) to refine the effective Hamiltonian parameters of $^{15}N_2^{16}O$ by using the most extensive compilation of the line position measurements available to date, (ii) to calculate accurate values of the $^{15}N_2^{16}O$ partition function and (iii) to construct a $^{15}N_2^{16}O$ room temperature line list. The paper is organized as follows. The polyad model of the effective Hamiltonian (H^{eff}) is outlined in Section 2. The global fitting of the H^{eff} parameters to the measured line positions of $^{15}N_2^{16}O$ is discussed in Section 3. In Section 4 the room temperature line list is presented. The conclusions are given in Section 5.

2. Effective Hamiltonian

The polyad model of H^{eff} describing globally the N_2O vibrational–rotational states in the ground electronic state of nitrous oxide has been suggested by Pliva [30] and developed by Teffo and Chedin [16]. A reduced model of this Hamiltonian was elaborated in Ref. [31] and extended on the sixth-order terms in Ref. [19]. The polyad model of H^{eff} is based on the polyad structure of the N_2O vibrational states resulting from the approximate relations between harmonic frequencies

$$\omega_1 \approx 2\omega_2 \quad \text{and} \quad \omega_3 \approx 4\omega_2 \tag{1}$$

The vibrational polyads are identified by the pseudo quantum number P:

$$P = 2V_1 + V_2 + 4V_3 \tag{2}$$

where V_1, V_2, and V_3 denote normal mode vibrational quantum numbers.

The H^{eff} could be presented by its matrix elements in the basis of harmonic oscillator and rigid symmetric top rotor eigenfunctions

$$|V_1V_2l_2V_3J\rangle = |V_1V_2l_2V_3J\rangle|JK=l_2\rangle, \quad (3)$$

where J is the total angular momentum quantum number, K is the quantum number of the projection of the total angular momentum on the molecular-fixed z-axis, and l_2 is the vibrational angular momentum quantum number. In order to reduce the size of the effective Hamiltonian matrix, it is common to introduce Wang-type basis functions:

$$|V_1V_2l_2V_3J\epsilon\rangle = \frac{1}{\sqrt{2}}(|V_1V_2l_2V_3J\rangle|JK=l_2\rangle + \epsilon|V_1V_2-l_2V_3J\rangle|JK = -l_2\rangle \quad (l_2\neq 0),$$
$$|V_1V_20V_3J\epsilon=1\rangle = |V_1V_20V_3J\rangle|JK=0\rangle \quad (l_2=0), \quad (4)$$

where $\varepsilon=1$ and -1 correspond to the so-called e and f levels, respectively. In this basis H^{eff} splits into independent blocks, each block being defined by three labels: P, the Wang parity $C=\{e,f\}$, and J. Thus, the eigenvalues of H^{eff} can be unambiguously labeled by four labels (P, C, J, and N), where N is the ranking index of eigenvalues in a (P, C, and J) block. These labels will be called the generalized nomenclature of an energy level.

In the process of the least-squares fits of $^{14}N_2^{16}O$ data several interpolyad interactions were found. They are not accounted for by the effective values of the effective Hamiltonian parameters. Indeed, an analysis of these interactions in $^{14}N_2^{16}O$ showed that they become pronounced for highly-excited states and affect rather weak transitions [19]. Expressions for the matrix elements of H^{eff} are given in Ref. [19].

3. Measured $^{15}N_2^{16}O$ data and the least-squares fitting

The file of experimental line positions used in Ref. [10] has been augmented with data from Refs. [7–14]. Most new data originate from FTS measurements performed at University of Science and Technology of China, Hefei, China. Gao et al. [11] has measured the line parameters of more than 6000 transitions of $^{15}N_2^{16}O$ in the 3500–9000 cm^{-1} region using a Bruker IFS 120HR interferometer equipped with a multi-pass gas cell and a $^{15}N_2^{16}O$-enriched sample. The accuracy of the unblended and not-very-weak lines estimated to be better than 0.001 cm^{-1}. Du et al. [13] has measured more than 7000 line positions in the 1650–3450 cm^{-1} range with a typical accuracy of 0.0005 cm^{-1} using the same experimental setup and a highly-enriched $^{15}N_2^{16}O$ sample. Song et al. [12] has measured 191 transitions of the weak 00061-00001 and 01161(2)-01101(2) bands using a CW-CRDS spectrometer operated near 0.8 μm. Estimated accuracies of the measurements were 0.001 cm^{-1} for the cold band and 0.002 cm^{-1} for the hot bands. Lyulin et al. [10] has measured 511 lines of 8 cold bands and one hot band lying between 5800 and 7600 cm^{-1} using the Bruker IFS 120 HR interferometer of the LADIR (Laboratoire de Dynamique, Interactions et Réactivité), Paris, France. The average absolute accuracy of the line positions has been estimated to be 0.0005 cm^{-1}.

Data from Refs. [7–9] were not used in the least-squares fit reported in Ref. [10]. Bauer et al. [7] has used a microwave setup and measured the line positions of five pure rotational lines with an uncertainty about 0.1 MHz. Toth [8,9] has measured line positions of the 10001-00001 and 00011-00001 bands with a typical uncertainty better than 0.0001 cm^{-1}. The line positions of Toth's sisam.n2o line list [14] are not truly measured values. They are calculated ones from the fitted spectroscopic constants G_v, B_v, D_v, and H_v of the measured bands. The estimated uncertainty of these data is about 0.0005 cm^{-1}.

The resulting data file included more than 18,000 entries and covered the 4–12,516 cm^{-1} spectral range. The H^{eff} parameters given in Table 7 of Ref. [16] reproduce these data with an RMS deviation 0.28 cm^{-1}. In this work the parameters of H^{eff} were fitted to the measured line positions with the GIP computer code [32]. The goal of the fitting is to minimize the dimensionless standard deviation defined according to the usual formula

$$\chi = \sqrt{\sum_i \left(\frac{obs_i - calc_i}{\delta_i}\right)^2 / (N-n)} \quad (5)$$

where obs_i and $calc_i$ are observed and calculated values of the i-th line position, respectively, δ_i is the measurement uncertainty, N is the number of fitted values, and n is the number of adjusted H^{eff} parameters. With 109 parameters we were able to reach $\chi=1.31$. Overall number of the fitted line positions was 18,013 and the number of energy levels was 5723. The reached χ value does mean that global fitting of vibrational–rotational line positions has been performed near experimental accuracy. This result is confirmed by the value of 0.0011 cm^{-1} obtained for the RMS deviation between calculated and experimental positions. The residuals $obs_i - calc_i$ are plotted versus the wavenumber in Fig. 1.

One can see from this figure that the residuals are randomly scattered around the $Y=0$ axis. This means that there is no manifestation of interpolyad resonance interactions between energy levels and that the polyad H^{eff} model is adequate to the fitted data. The percentage of residuals being within ± 0.0001 cm^{-1}, ± 0.0005 cm^{-1}, ± 0.001 cm^{-1}, and ± 0.005 cm^{-1} bounds is 15%, 55%, 80%, and 99%, respectively. The characteristics of the sources of the fitted data and the results of the fitting are summarized in Table 2. The values of the fitted H^{eff} parameters are given in the Supplementary material.

In order to calculate the line intensities at a given temperature it is necessary to know the value of the total partition function $Q(T)$. Direct summation over all calculated energy levels was carried out until convergence within a specified tolerance. The partition function was calculated for the 200–396 K temperature range with the state-independent degeneracy factor $g=4$. The highest polyad and J quantum number used in summation were 9 and 200, respectively. The total number of energy levels used in summation was 32,150. Relative accuracy of the

calculated $Q(T)$ values is better than 10^{-5}. Table 3 contains the values of $Q(T)$ in the 200–396 temperature range.

4. Room temperature $^{15}N_2^{16}O$ line list

In order to calculate a room temperature line list, which includes line positions, line intensities, lower state energies and labeling one needs a model of an effective dipole moment (D^{eff}) operator. In our effective operator approach D^{eff} is constructed in the same way as H^{eff}. The model leads to a serial approach. In the framework of this approach all vibrational bands of an isotopologue are divided into the series which do not cross over. Each series is determined by the value of $\Delta P = P' - P''$, where P' and P'' are polyad numbers of upper and lower states, respectively. The intensities of the lines belonging to a defined series depends on its own set of the D^{eff} parameters, which can be fitted to corresponding observed line intensities separately. Details of the D^{eff} model can be found in Ref. [20].

To our knowledge, there are only three sources of $^{15}N_2^{16}O$ line intensities. Toth's line list sisam.n2o [14] contains intensities of 424 lines of the 00011-00001, 01111-01101, 01112-01102, 10001-00001, 10011-00001, and 20001-00001 bands. However, they are not truly measured values. They are calculated ones from the fitted band intensity and Herman-Wallis parameters. Song et al. [12] reported measured intensities of the 00061-00001 and 01161(2)-01101(2) bands with estimated uncertainty of 4%. Lyulin et al. [10] has measured the line positions and intensities of 511 lines of 8 cold bands 30011-00001, 50001-00001, 42001-00001, 00031-00001, 20021-00001, 40011-00001, 32011-00001, 10031-00001, and one hot band 01131(2)-01101(2) lying between 5800 and 7600 cm^{-1}. However, to calculate a line list we need also D^{eff} parameters for other ΔP series, like the $\Delta P = 1,3$, etc. For this purpose, we can use the parameters of the fitted D^{eff} models of the principal isotopologue $^{14}N_2^{16}O$ along with the fitted $^{15}N_2^{16}O$ H^{eff} model to calculate intensities of $^{15}N_2^{16}O$. This approach was justified by the fact that the lower order D^{eff} parameters of CO_2 are practically independent on isotopologue [33] in the case of a substitution which does not change permutation symmetry of the molecule. This is also confirmed by the fitted values of the vibrational transition dipole moments squared for the 00061-00001 bands of two nitrous oxide isotopic species: $^{14}N_2^{16}O$ and $^{15}N_2^{16}O$ [12,34].

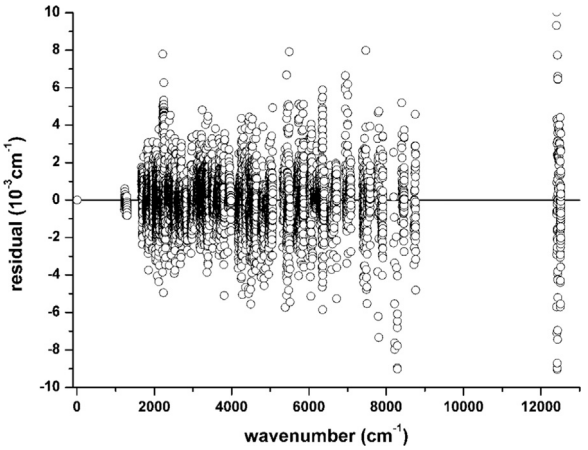

Fig. 1. Residuals between observed and calculated line positions of $^{15}N_2^{16}O$ versus wavenumber.

The effective dipole moment parameters of $^{14}N_2^{16}O$ were obtained in Refs. [20–27]. For the $\Delta P = 2,3,4,5,6$ series, the pure vibrational parameters of D^{eff} were obtained in Ref. [20]. These parameters were fitted to the published band intensities. Later, parameters of D^{eff} for the $\Delta P = 4$ series were refitted to measured line intensities [21]. Daumont et al. have fitted the parameters of the D^{eff} models to the measured $^{14}N_2^{16}O$ intensities of the $\Delta P = 2$ [22], $\Delta P = 7–9$, [23] and $\Delta P = 10–14,16,18$ [24] series. For the $\Delta P = 0–1$ series, the fitted parameters of the D^{eff} were reported in Ref. [27].

In order to check isotopic extrapolation properties of the fitted $^{14}N_2^{16}O$ dipole moment parameters, we calculated the intensities of the bands given in Refs. [10,14] using the fitted $^{15}N_2^{16}O$ H^{eff} parameters and the fitted dipole moment parameters of $^{14}N_2^{16}O$. The calculated values were compared with the measured ones. The residuals defined as $100\%*(I_{obs} - I_{calc})/I_{obs}$ versus the wavenumber are plotted in Fig. 2. As one can see from this figure, practically all intensities of the strong bands, which are defined by the lower order D^{eff} parameters, are

Table 2
Experimental data and statistics of the global fit of $^{15}N_2^{16}O$ line positions.

Reference	Setup[a]	Spectral domain (cm^{-1})	J_{max}[b]	Uncertainty[c] (10^{-3} cm^{-1})	N_{fit}[d]	RMS[e] (10^{-3} cm^{-1})
Amiot et al. [6]	FTS	3631–6396	61	1.0	1306	0.8
Bauer et al. [7]	MW	4.0485–7.2870	9	0.003	5	0.002
Toth [8,9]	FTS	1229–2183	53	0.1	76	0.2
Toth [14]	FTS	1227–3414	54	1.0	423	0.7
Lyulin et al. [10]	FTS	5814–7582	44	0.5	509	0.6
Gao et al. [11]	FTS	1682–8760	90	1.0	8736	1.2
Du et al. [13]	FTS	1668–3397	100	0.5	6814	0.8
Song et al. [12]	CW-CRDS	12401–12516	50	1.0–2.0	142	4.4

[a] FTS – Fourier transform spectrometer, MW – microwave spectrometer, CW-CRDS – continuous-wave cavity ring-down spectrometer.
[b] Maximal value of the rotational quantum number.
[c] Uncertainties of the measured line positions as given in the references.
[d] Number of fitted lines.
[e] RMS of residuals.

Table 3
Partition function of $^{15}N_2^{16}O$.

T	Q(T)	T	Q(T)	T	Q(T)	T	Q(T)	T	Q(T)
200	1421.1	240	1763.0	280	2148.7	320	2587.0	360	3086.0
204	1453.6	244	1799.4	284	2190.0	324	2634.0	364	3139.5
208	1486.4	248	1836.3	288	2231.9	328	2681.7	368	3193.7
212	1519.6	252	1873.7	292	2274.3	332	2729.9	372	3248.7
216	1553.2	256	1911.5	296	2317.2	336	2778.8	376	3304.3
220	1587.1	260	1949.8	300	2360.7	340	2828.4	380	3360.7
224	1621.5	264	1988.6	304	2404.8	344	2878.6	384	3417.8
228	1656.2	268	2027.8	308	2449.5	348	2929.4	388	3475.6
232	1691.4	272	2067.6	312	2494.7	352	2980.9	392	3534.2
236	1727.0	276	2107.9	316	2540.5	356	3033.1	396	3593.5

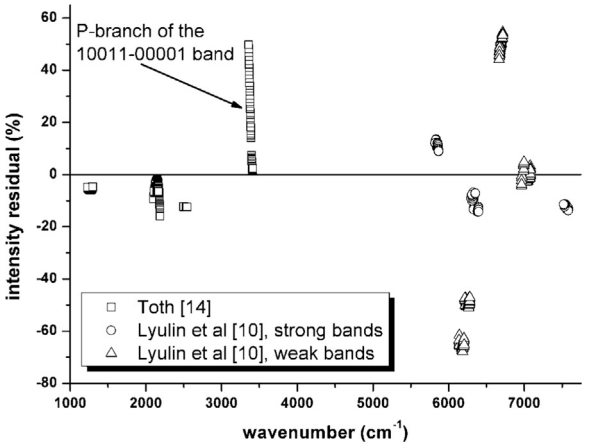

Fig. 2. Comparison of our calculated ($^{15}N_2^{16}O$ line list) and the measured line intensities.

consistent with our calculated values within 20%. The only exception is the P-branch of the 10011-0001 band. The unusual behavior of the P-branch is caused by an anharmonic perturbation of the 10011 state by the 14001 state that has not been taken into account during the generation of the sisam.n2o line list.

In order to create the $^{15}N_2^{16}O$ linelist we performed least squares fittings of the $^{15}N_2^{16}O$ D^{eff} parameters for the ΔP=2,4,6,10,12,14 series using measured data from Refs. [10,14]. The average absolute accuracy of the measured line intensities reported in Ref. [10] has been estimated to be 2–5%. Toth's sisam.n2o line list [14] includes data of eight most abundant isotopic species. The data of five most abundant species were included in the HITRAN database [2]. All these data have 6 as the uncertainty code of the intensities. According to HITRAN conventions, this means that estimated uncertainty of the intensities is between 2% and 5%. We believe that the $^{15}N_2^{16}O$ sisam.n2o intensities have similar interval of the uncertainties. Taking all this into account, we assigned 5% to all data from Refs. [10,14] as the uncertainties of the measured intensities. The values of $^{14}N_2^{16}O$ D^{eff} parameters for the ΔP=2,4,6,10,12,14 series of transitions reported in Refs. [21–24] were used as initial guesses. During the fitting we varied only those parameters which influence on experimental line intensities of $^{15}N_2^{16}O$.

Table 4
Summary of the $^{15}N_2^{16}O$ line intensity fits.

ΔP	Reference	N_{fit}[a]	N_{band}[b]	J_{max}[c]	N_{par}[d]	RMS[e] extrapol	RMS[e] fit
2	Toth [14]	86	1	44	1	5.1	0.2
4	Toth [14]	278	3	54	3	7.7	2.0
6	Toth [14]	28	1	35	1	23.4	1.6
10	Lyulin et al. [10]	181	3	42	3	50.9	1.9
12	Lyulin et al. [10]	170	4	42	4	24.7	1.8
14	Lyulin et al. [10]	51	1	38	1	12.5	0.7

[a] Number of fitted lines.
[b] Number of fitted bands.
[c] Maximal value of the rotational quantum number.
[d] Number of fitted D^{eff} parameters.
[e] Root mean square of the 100%*($S_{obs}-S_{calc}$)/S_{obs} value.

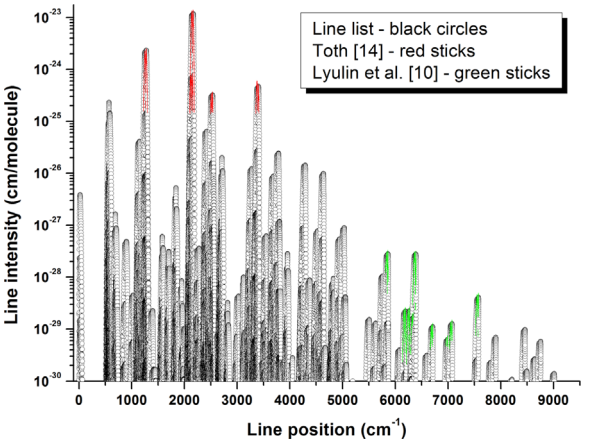

Fig. 3. Graphical overview of the $^{15}N_2^{16}O$ line list and the measured data from Refs. [10,14].

For the ΔP=0,1,3,5,7,8,9,11,13,16 series we used the $^{14}N_2^{16}O$ D^{eff} parameters. In both cases the new set of the $^{15}N_2^{16}O$ effective Hamiltonian parameters was used for the calculation of the line intensities. Results of the least squares fittings of the D^{eff} parameters for the ΔP=2,4,6,10,12,14 series are summarized in Table 4. For each series we were able to obtain RMS deviation of the fit less than estimated uncertainties of the fitted intensities.

The values of the D^{eff} parameters are given in the Supplementary material.

We used a reference temperature 296 K, an intensity cut off 10^{-30} cm/molecule, and the natural abundance 1.32×10^{-5} to calculate a $^{15}N_2^{16}O$ line list. The partition function value for 296 K was taken from Table 2. A graphical overview of the line list and the measured data from Refs. [10,14] are given in Fig. 3.

We estimate the accuracy of the line list positions to be 0.001–0.01 cm^{-1}. Taking into account uncertainties of the fitted $^{15}N_2^{16}O$ intensities of the ΔP=2,4,6,10,12,14 series, we estimate the accuracy of the line list intensities of these series to be about 5%. The accuracy of the line list intensities of the ΔP=0,1,3,5,7,8,9,11,13,16 series in the case of strong bands to be about 20%. The uncertainty of the line intensities of all other bands may reach 100%.

5. Conclusion

The $^{15}N_2^{16}O$ line positions collected from the literature have been modeled using a polyad model of effective Hamiltonian. The fitted model is able to reproduce known measured line positions with accuracies compatible with the measurement uncertainties. The set of 109 effective Hamiltonian parameters was fitted to 18,013 observed line positions with dimensionless weighted standard deviation equal to 1.31. The fitted set of parameters reproduces the line positions involved in to the fit with RMS= 0.0011 cm^{-1}.

Accurate values of the total partition function have been calculated for the 200–396 K temperature range.

A list of $^{15}N_2^{16}O$ line positions and intensities (at 296 K) together with spectroscopic labeling of the energy levels was generated. The intensity cutoff was set to 10^{-30} cm/molecule. The line list is based on the fitted polyad model of effective Hamiltonian for $^{15}N_2^{16}O$ obtained in the present work, and the parameters of the effective dipole moment operators reported in the literature for $^{14}N_2^{16}O$. For the series ΔP=2,4,6,10,12,14, some low order effective dipole moment parameters were determined by fitting line intensities reported in the literature for $^{15}N_2^{16}O$. We estimate the uncertainties of the line list positions to be 0.001–0.01 cm^{-1} and the uncertainties of the line list intensities of strong bands to be about 5–20%, depending of the ΔP series. The uncertainties of the weak bands could be considerably higher. The line list is available as the Supplementary material. Additional information concerning the values of the fitted experimental line positions and intensities and their residuals as well as comparisons for the other experimental data discarded from the fits can be obtained upon request to the corresponding author.

Acknowledgments

This work is jointly supported by the NSFC (21225314, 21303176, and 21473172), RFBR (Russia, grant no. 14-05-91150), and by the Government of the Russian Federation in frame of contract no. 02.A03.21.0006, Act 211.

Appendix A. Supplementary material

Supplementary data associated with this article can be found in the online version at http://dx.doi.org/10.1016/j.jqsrt.2016.01.038.

References

[1] Berglund M, Wieser ME. Isotopic compositions of the elements 2009 (IUPAC Technical Report). Pure Appl Chem 2011;83:397–410.
[2] Rothman LS, Gordon IE, Babikov Y, Barbe A, Benner DC, Bernath PF, et al. The HITRAN 2012 molecular spectroscopic database. J Quant Spectrosc Radiat Transf 2013;130:4–50.
[3] Stein LY, Yung YL. Production, isotopic composition, and atmospheric fate of biologically produced nitrous oxide. Annu Rev Earth Planet Sci 2003;31:329–56.
[4] Eiler JM. The isotopic anatomies of molecules and minerals. Annu Rev Earth Planet Sci 2013;41:411–41.
[5] Waechter H, Mohn J, Tuzson B, Emmenegger L, Sigrist MW. Determination of N_2O isotopomers with quantum cascade laser based absorption spectroscopy. Opt Express 2008;16:9239–44.
[6] Amiot C. Vibration-rotation bands of $^{15}N_2^{16}O$–$^{14}N_2^{18}O$. J Mol Spectrosc 1976;59:380–95.
[7] Bauer A, Teffo JL, Valentin A, McCubbin TK. The ground state rotational constants of $^{15}N^{15}N^{16}O$. J Mol Spectrosc 1986;120:449–54.
[8] Toth RA. Frequencies of N_2O in the 1100- to 1440-cm^{-1} region. J Opt Soc Am B 1986;3:1263–81.
[9] Toth RA. N_2O vibration–rotation parameters derived from measurements in the 900–1090- and 1580–2380-cm^{-1} regions. J Opt Soc Am B 1987;4:357–74.
[10] Lyulin OM, Jacquemart D, Lacome N, Tashkun SA, Perevalov VI. Line parameters of $^{15}N_2^{16}O$ from Fourier transform measurements in the 5800–7600 cm^{-1} region and global fitting of line positions from 1000 to 7600 cm^{-1}. J Quant Spectrosc Radiat Transf 2010;111:345–56.
[11] Gao B, Wang C-Y, Liu Y, Liu A-W, Hu S-M. High-resolution infrared spectroscopy of $^{15}N_2^{16}O$ in the 3500–9000 cm^{-1} region. J Mol Spectrosc 2010;259:20–5.
[12] Song K-F, Gao B, Liu A-W, Perevalov VI, Tashkun SA, Hu S-M. Cavity ring-down spectroscopy of the $6v_3$ bands of ^{15}N substituted N_2O. J Quant Spectrosc Radiat Transf 2010;111:2370–81.
[13] Du J-H, Liu A-W, Perevalov VI, Tashkun SA, Hu S-M. High-resolution infrared spectroscopy of $^{15}N_2^{16}O$ in 1650–3450 cm^{-1}. Chin J Chem Phys 2011;24:611–9.
[14] Toth RA. ⟨http://mark4sun.jpl.nasa.gov/n2o.html⟩.
[15] Jacquinet-Husson N, Crepeau L, Armante R, Boutammine C, Chedin A, Scott NA, et al. The 2009 edition of the GEISA spectroscopic database. J Quant Spectrosc Radiat Transf 2011;112:2395–445.
[16] Teffo JL, Chedin A. Internuclear potential and equilibrium structure of the nitrous oxide molecule from rovibrational data. J Mol Spectrosc 1989;135:389–409.
[17] Schroder B, Sebald P, Stein C, Weser O, Botschwina P. Challenging high-level *ab initio* rovibrational spectroscopy: the nitrous oxide molecule. Z Phys Chem 2015;229:1663–90.
[18] Zúñiga J, Bastida A, Requena A. Theoretical vibrational terms and rotational constants for the ^{15}N substituted isotopologues of N_2O calculated using normal hyperspherical coordinates. J Quant Spectrosc Radiat Transf 2012;113:26–46.
[19] Perevalov VI, Tashkun SA, Kochanov RV, Liu AW, Campargue A. Global modeling of the line positions of $^{14}N_2^{16}O$ within the framework of the polyad model of effective Hamiltonian. J Quant Spectrosc Radiat Transf 2012;113:1004–12.
[20] Lyulin OM, Perevalov VI, Teffo JL. Effective dipole moment and band intensities of nitrous oxide. J Mol Spectrosc 1995;174:566–80.
[21] Lyulin OM, Perevalov VI, Teffo JL. Fitting of line intensities using the effective operator approach: the 4 μm region of $^{14}N_2^{16}O$. J Mol Spectrosc 1996;180:72–4.
[22] Daumont L, Claveau C, De Backer-Barilly MR, Hamdouni A, Regalia-Jarlot LR, Teffo JL, et al. Line intensities of $^{14}N_2^{16}O$: the10 μm region revisited. J Quant Spectrosc Radiat Transf 2002;72:37–55.
[23] Daumont L, Vander Auwera J, Teffo JL, Perevalov VI, Tashkun SA. Line intensity measurements in $^{14}N_2^{16}O$ and their treatment using the effective dipole moment approach. I. The 4300 to 5200 cm^{-1} region. J Mol Spectrosc 2001;208:281–91.

[24] Daumont L, Vander Auwera J, Teffo JL, Perevalov VI, Tashkun SA. Line intensity measurements in $^{14}N_2^{16}O$ and their treatment using the effective dipole moment approach. II. The 5400–11,000 cm^{-1} region. J Quant Spectrosc Radiat Transf 2007;104:342–56.
[25] Karlovets EV, Lu Y, Mondelain D, Kassi S, Campargue A, Tashkun SA, Perevalov VI. High sensitivity CW-Cavity Ring Down Spectroscopy of N_2O between 6950 and 7653 cm^{-1} (1.44–1.31 μm): II. Line intensities. J Quant Spectrosc Radiat Transf 2013;117:81–7.
[26] Karlovets EV, Campargue A, Kassi S, Perevalov VI, Tashkun SA. High sensitivity Cavity Ring Down Spectroscopy of N_2O near 1.22 μm: (I) rovibrational assignments and band-by-band analysis. J Quant Spectrosc Radiat Transf 2016;169:36–48.
[27] Tashkun SA, Perevalov VI, Lavrentieva NN. NOSD-1000, the high-temperature nitrous oxide spectroscopic databank. J Quant Spectrosc Radiat Transf 2015. http://dx.doi.org/10.1016/j.jqsrt.2015.11.014.
[28] Tashkun SA, Perevalov VI, Kochanov RV, Liu A-W, Hu S-M. Global fittings of $^{14}N^{15}N^{16}O$ and $^{15}N^{14}N^{16}O$ vibrational–rotational line positions using the effective Hamiltonian approach. J Quant Spectrosc Radiat Transf 2010;111:1089–105.
[29] Vlasova AV, Perevalov BV, Tashkun SA, Perevalov VI. Global fittings of the line positions of the rare isotopic species of the nitrous oxide molecule. In: Proceedings of the XVth symposium on high-resolution molecular spectroscopy. SPIE (Nizhny Novgorod, Russia); 2006, vol. 6580. p. 658007.
[30] Pliva J. Molecular constants of nitrous oxide. $^{14}N_2^{16}O$. J Mol Spectrosc 1968;27:461–88.
[31] Teffo JL, Perevalov VI, Lyulin OM. Reduced effective Hamiltonian for global treatment of rovibrational energy levels of nitrous oxide. J Mol Spectrosc 1994;168:390–403.
[32] Tashkun SA, Perevalov VI, Teffo J-L, Rothman LS, Tyuterev VlG. Global fitting of $^{12}C^{16}O_2$ vibrational–rotational line positions using the effective Hamiltonian approach. J Quant Spectrosc Radiat Transf 1998;60:785–801.
[33] Karlovets EV, Perevalov VI. Calculation of the carbon dioxide effective dipole moment parameters of the qJ and q^2J types for rare isotopologues. Atmos Ocean Opt 2011;24:101–6 [in Russian].
[34] Milloud R, Perevalov VI, Tashkun SA, Campargue A. Rotational analysis of $6\nu_3$ and $6\nu_3+\nu_2-\nu_2$ bands of $^{14}N_2^{16}O$ from ICLAS spectra between 12760 and 12900 cm^{-1}. J Quant Spectrosc Radiat Transf 2011;112:553–7.